

# **Microstructure and mechanical properties of diffusion bonded joints between tungsten and F82H steel using a titanium interlayer**

Zhihong Zhong<sup>1</sup>, Tatsuya Hinoki<sup>2,\*</sup>, Takashi Nozawa<sup>3</sup>, Yi-Hyun Park<sup>2</sup>, and Akira Kohyama<sup>2,+</sup>

<sup>1</sup> Graduate School of Energy Science, Kyoto University, Gokasho, Uji, Kyoto 611-0011, Japan

<sup>2</sup> Institute of Advanced Energy, Kyoto University, Gokasho, Uji, Kyoto 611-0011, Japan

<sup>3</sup> Japan Atomic Energy Agency, 2-4 Shirakata Shirane, Tokai, Ibaraki 319-1195, Japan

<sup>+</sup> Present address: College of Design and Manufacturing Technology, Muroran Institute of Technology, 27-1 Mizumoto-cho, Muroran 050-8585, Japan

## **Abstract:**

Diffusion bonding between W and ferritic/martensitic steel F82H using a Ti interlayer was carried out in vacuum at temperature range of 850–950 °C for 1 h with 10 MPa. Metallographic analysis with field-emission scanning electron microscopy revealed excellent bonding at both W/Ti and Ti/F82H interfaces. The chemical compositions of the reaction products were analyzed by energy dispersive spectroscopy and their existence were confirmed by X-ray diffraction technique.  $\alpha$ - $\beta$  Ti solid solution was detected at W/Ti interface, while the reaction phases at Ti/F82H interface are dependent on the joining temperature. Joint strength was evaluated and the variations in strength of the joints were significantly related to the microstructural evolution of the diffusion zone. All the joints fractured at Ti/F82H interface during shear testing. The hardness distribution across the joining interfaces was also determined.

**Keywords:** Diffusion bonding; Tungsten; Steel; Titanium; Microstructure

---

\* Corresponding author: Tel: +81-774-383465; Fax: +81-774-383467.  
E-mail:zh\_zhong@iae.kyoto-u.ac.jp (Z. Zhong); hinoki@iae.kyoto-u.ac.jp (T. Hinoki)

## 1. Introduction

Tungsten (W) is a promising refractory material for fusion nuclear application, for its high resistance against sputtering and low tritium retention [1,2]. Reduced activation ferritic/martensitic (RAFM) steels, which were developed for simplify special waste storage of highly radioactive structures of fusion reactor after service, is one of the candidates to be used as first wall and blanket structural materials in fusion reactors [3], F82H is one such steel [4]. Joining of W to RAFM steels is required for some components such as divertor in fusion device according to the design [5]. Conventional fusion welding method is inapplicable for joining of them, due to a high possibility of the brittle intermetallic compounds ( $\text{FeW}$  and  $\text{Fe}_7\text{W}_6$ ) formation in the weld zone, in addition the large difference in melting points of these two materials. Furthermore, W and steel have remarkable differences in their physical properties, in particular the mismatch of their coefficients of thermal expansion (CTE), which results in a large residual stress in the joints after joining.

Several joining techniques have been developed for joining of W to steel, such as active metal brazing [6], plasma spraying [7], and diffusion bonding [8,9]. The metallic brazing produced high strength joints and provided well reproducible results. However, the brazing temperature of 1150 °C is high enough to cause grain coarsening in steel and consequently leads to the degradation of material's properties [6]. For the components produced by plasma spraying, obtaining an acceptable dense and sufficient strength W coating on steel is difficult. Diffusion bonding seems to be a suitable way to join W with steel due to its tolerable bonding temperature and the joint could be used at

high temperatures.

In the case of diffusion bonding of dissimilar materials, an interlayer inserted between substrates is often necessary to prevent the formation of intermetallic compound and to reduce the residual stress in the joints. We have successfully used nickel as interlayer for bonding of W to ferritic steel and found that the tensile strength of the joint was as high as 215 MPa [9]. In the present work, we investigated the feasibility of joining of W to F82H steel by inserting a titanium (Ti) interlayer through diffusion bonding. Ti was selected as interlayer material because the CTE of Ti ( $8.4 \times 10^{-6} \text{K}^{-1}$ ) is between that of W ( $4.5 \times 10^{-6} \text{K}^{-1}$ ) and F82H steel ( $12.3 \times 10^{-6} \text{K}^{-1}$ ) which is expected to help mitigate the residual stress in the joint, as well as it forms continuous solid solution with W. In addition, Ti has low activation characteristic which is attractive for fusion nuclear applications.

## 2. Experimental procedures

The commercially available W and IEA (International Energy Agency) heated F82H steel used in this work were cut by a diamond saw to a dimension of  $10^{\text{L}} \times 5^{\text{W}} \times 2^{\text{T}} \text{ mm}^3$  from the as-received plates. A 0.6 mm thick commercial Ti sheet was cut to a size of  $10^{\text{L}} \times 5^{\text{W}} \text{ mm}^2$ . The chemical compositions of these materials are given in Table 1. Prior to diffusion bonding, the bonding surface of all materials was polished by an emery paper with 1500 grit. The materials were then cleaned in an ultrasonic bath using acetone for 10 min and finally dried in air. The assembly of W/Ti/F82H was joined in a hot-press furnace with a heating rate of  $10 \text{ }^{\circ}\text{C/min}$ , at temperature range of  $850\text{--}950 \text{ }^{\circ}\text{C}$  for 1 h

under a load of 10 MPa in vacuum ( $<5.0 \times 10^{-3}$  Pa). Once the bonding process was completed, removed the load, and the joint was cooled at a rate of 5 °C/min to 400 °C and followed by furnace cooling in vacuum to room temperature.

The cross-sections of diffusion bonded joints were perpendicularly cut and prepared for metallographic examination by polishing down to 1  $\mu\text{m}$  finish. The microstructure observation was carried out in a field-emission scanning electron microscope (FE-SEM, JEOL JSM 6700). Chemical composition of the reaction phase was analyzed with energy dispersive X-ray spectrometry (EDS) attached to FE-SEM. The reaction phase was confirmed by X-ray diffraction (XRD) using a Cu  $K_{\alpha}$  radiation source. The elemental intensity profiles of the chemical species across the interface were drawn from the electron probe microanalysis (EPMA). The LiF crystal was utilized to generate the corresponding  $K_{\alpha}$  lines of Fe, Cr and Ti, and  $M_{\alpha}$  line of W. Mechanical properties of the joint were evaluated by shear strength and hardness tests. The joint strength test was performed at room temperature using a tensile-testing machine (Instron 5581) at a crosshead speed of 0.5 mm/min with a specimen size of  $3^L \times 3^W \times 4.5^T \text{ mm}^3$  in a specially designed jig. Five samples were tested for each processing. Fracture surface after shear testing was observed under FE-SEM. Hardness profile across the bonding interface was determined by a nano-indenter (ENT-1100a) with a load of 10 g.

### **3. Results and discussion**

#### *3.1. Microstructural and morphological analysis*

Successful solid-state diffusion bonding was achieved between W and F82H steel

using a Ti interlayer under all the employed experimental conditions. Fig. 1 shows a typical general view of the transition joint bonded at 900 °C. Both W/Ti and Ti/F82H interfaces are free from discontinuities or cracks. Figs. 2(a) through (c) are the back-scattered electron images (BEIs) of W/Ti interfaces for the joints bonded at 850, 900, and 950 °C, respectively. In all images, the left part with light-gray contrast is W and the right part with deep-gray contrast is Ti. It can be obviously recognized from the color contrast that a diffusion zone was formed between W and Ti. All the interfaces show similar layered structures, but the thickness of diffusion zone grows from ~2 to ~12  $\mu\text{m}$  corresponding to the joining temperature increases from 850 to 950 °C, indicating that the atomic interdiffusion was enhanced at higher temperature. In addition, some transverse micro-cracks can be observed at the W/Ti interface for the joint bonded at 950 °C. The formation of these cracks may be attributed to the following reasons: (1) the CTE mismatch between W and F82H; (2) the enhanced interaction between W and Ti; (3) the CTE mismatch between W and Ti. Considering that crack was not observed for the both 850 and 900 °C joints, the effect of CTE mismatch between W and Ti on the crack formation is believed to be minimal. A likely explanation is that the enhanced interaction between W and Ti, which in turn gives rise to cracking due to the different atomic sizes of W and Ti. This justification, however, does not exclude the effect of CTE mismatch between W and F82H, because the residual stress that developed in the dissimilar materials joint proportionally increases with the temperature difference between joining and room temperature [10]. The higher the joining temperature, the larger residual stresses may generate in the joint. Nevertheless, these transverse cracks would not greatly affect the joint compressive shear strength, see the after presented strength test results.

Figs. 3(a) through (c) show the elemental intensity profiles obtained by line-scan analysis of EPMA across the W/Ti interface for the joints bonded at 850, 900, and 950 °C, respectively. From Fig. 3, the profiles curves vary continuously and smoothly across the interface, suggesting that solid solution was formed at the W/Ti interface. The penetration depth of W in Ti is much higher than that of Ti in W and increased as the joining temperature increased. One may notice that the profile curves are somewhat irregular in the diffusion zone near Ti, which is due to the mixed phases in the diffusion zone. The brighter needles in the diffusion zone are relatively rich W content and the darker ones are Ti-rich region (see Fig. 2). Combining with the EPMA results shown in Fig. 3, the overall cross-sectioned microstructure of W/Ti interface can be generalized into three regions from W to Ti corresponding to (1) W, (2) the  $\beta$ -W–Ti solid solution with transformed  $\alpha$ -Ti and (3)  $\alpha$ -Ti.

The formation of solid solution between W and Ti is expected on the basis of the W–Ti phase diagram which shows complete solubility in the  $\beta$ -region [11]. Obviously, the diffusion zone shown in Fig. 2 is the consequence of the atomic interdiffusion between W and Ti, and was developed as a result of eutectoid transformation. An adequate amount of W in this zone promoted the eutectoid formation of Ti by decreasing the  $\alpha$ - $\beta$  transformation temperature [12], thus the observed brighter  $\beta$ -Ti needles containing W were transformed in the darker  $\alpha$ -Ti matrix by the decomposition of  $\beta$ -Ti during cooling. The width of this Widmanstätten  $\alpha$ - $\beta$  structure zone increased as joining temperature increased, due to the enhanced interdiffusion. It has been noted that W atom diffused more distant in Ti than Ti atom did in W for all the joints. This feature could be explained by the higher diffusivity of W in Ti which is three orders of

magnitude higher than that of Ti in W [13].

Figs. 4(a) through (c) are the BEIs of Ti/F82H interface for the joints bonded at 850, 900, and 950 °C, respectively. The left part with dark-gray contrast is Ti and the right part with light-gray contrast is F82H. The elemental intensity profiles of Fe, Cr, W, and Ti across the diffusion zone are presented in Fig. 5. A very limited interdiffusion occurred for the joint bonded at 850 °C. However, when the bonding temperature was raised to above 900 °C, a marked difference in microstructure can be observed as compared with 850 °C joint. Adjacent to Ti, similar like that of W/Ti interface, a  $\alpha$ - $\beta$  Ti zone is composed of the light-gray strips and dark-gray  $\alpha$ -Ti matrix was found. Close to  $\alpha$ - $\beta$  Ti, a shade zone has been observed, which is enriched with Ti (~91 at. %) with small amounts of Fe (~8 at. %) and Cr (~1 at. %). This suggests that Fe and Cr from F82H penetrated into Ti. Fe and Cr atoms are strong  $\beta$ -phase stabilizers for Ti [14], and their appropriate quantities help to retain high-temperature  $\beta$ -structure; hence, in this area the high-temperature body centered cubic (bcc) phase of Ti has been retained after joining and was designated as retained  $\beta$ -Ti. The width of the retained  $\beta$ -Ti regions increased with increasing the joining temperature was also observed (Figs. 4(b) and (c)). Next to  $\beta$ -Ti, a small zone which contains Ti (~58 at. %), Fe (~40 at. %), and Cr (~2 at. %) was detected. From the isothermal section of Fe-Cr-Ti ternary phase diagram [15], it can be predicted that this zone probably consists of FeTi and  $\beta$ -Ti [16]. Between FeTi+ $\beta$ -Ti and F82H, a thin bright zone was found, which contains Fe (~60 at. %) and Ti (~30 at. %) in association with Cr (~7 at. %) and W (~3 at. %). This composition was determined to be the  $\lambda$  phase containing small amount of W in this zone, the  $\lambda$  phase is the solid solution of Fe<sub>2</sub>Ti and Cr<sub>2</sub>Ti [17]. Ti (< 10 at. %) also was found to penetrate

into F82H with some distance (10–30  $\mu\text{m}$ ) and this region, presumably, was  $\alpha$ -Fe phase retained from high temperature. The waved nature of Ti concentration curve in F82H side indicates that titanium atom may segregate at the grain boundaries of  $\alpha$ -Fe and the  $\chi$  phase ( $\text{Fe}_{17}\text{Cr}_7\text{Ti}_5$ ) may form in F82H.

From Figs. 4 and 5, it is evident that a rise in the joining temperature promotes the abundant diffusion of chemical species across the bonding interface. At Ti/F82H interface, the width of the diffusion zone is largely increased at 900 °C in comparison with 850 °C. At 850 °C, Ti and F82H have hexagonal close-packed (hcp) and face centered cubic (fcc) structures, respectively, and both of them are close-packed crystals. Therefore, their interdiffusion was limited. At 900 °C, however, F82H retained its fcc structure whereas Ti undergone a phase transformation from  $\alpha$ (hcp) to  $\beta$ (bcc) as this temperature is above the  $\beta$ -transus of Ti (882 °C). Owing to the more open crystallography of bcc structure, Fe and Cr atoms can migrate easier into  $\beta$ -Ti than into  $\alpha$ -Ti matrix, in addition the promotion of the high activity of chemical species at higher temperature. Thus substantial diffusion occurred across the interface. Due to the faster diffusion rate of Fe in Ti than that of Ti in Fe [18], Fe atom penetrated a longer distance into Ti and a thicker  $\alpha$ - $\beta$  Ti +  $\beta$ -Ti zone was observed compared to  $\alpha$ -Fe zone. Additionally, a  $\sigma$ -phase enriched in Cr (~30 wt. %) that resulted from the uphill diffusion of Cr was widely detected in the both Ti/steel [14,19,20] and Ti alloy/steel [17] interfaces. In the present study, however, the  $\sigma$ -phase has not been found due probably to the Cr concentration in F82H (7.7 wt. %) is much lower than that of in conventional stainless steel, for example, 304 stainless steel contains more than 18 wt. % Cr.



Fig. 6 shows the XRD pattern of the fracture surface on Ti side for the joint bonded at 950 °C. The reaction products in the Ti/F82H diffusion zone have been confirmed by XRD analysis. The  $\alpha$ -Ti, stabilized  $\beta$ -Ti, intermetallic phases of FeTi, Fe<sub>2</sub>Ti, and Cr<sub>2</sub>Ti, and oxide of Fe<sub>2</sub>Ti<sub>4</sub>O were identified on the fracture surface. The presence of Fe<sub>2</sub>Ti<sub>4</sub>O was not revealed by SEM analysis maybe due to its low volume fraction. The dissolved oxygen in titanium promotes the formation of oxide [21]. The necessary oxygen for the formation of Fe<sub>2</sub>Ti<sub>4</sub>O probably results from: (1) that dissolved in as-received Ti during processing; (2) the free surfaces of being joined metals during the diffusion couple preparation; and (3) that absorbed from the hot-press furnace chamber during joining process, due to the high affinity of Ti for oxygen.

### *3.2. Mechanical properties evaluation and fracture surface analysis*

Shear strength of the W/Ti/F82H joints is presented in Fig. 7. The strength increased when the joining temperature increased from 850 to 900 °C. For the low bonding temperature of 850 °C, the width of diffusion zone is small and the extent of interfacial deformation remains incomplete, as well as the interdiffusion of chemical species is limited at both interfaces. As a result, the mating surface is lack of contact and produced low strength joint. On the contrary, for the 900 °C joining temperature, betterment in plastic deformation of the mating surface improves contact quality. In particular, the extent of interdiffusion of chemical species was significantly enhanced at higher temperature. Thus the shear strength improved and reaches its maximum level ( $102 \pm 11$  MPa) for 900 °C joint, although a small width intermetallic layer was generated at the

Ti/F82H interface.

A further rise in joining temperature though leads to enhancement of interdiffusion and better plastic deformation, shear strength was decreased. Benefit from interdiffusion and detriment effect by the growth of brittle intermetallics may balance each other; and it seems that the shear strength is mainly governed by the latter factor. Additionally, the Kirkendall voids formed at the interface due to the imbalance in flux transfer of Ti and Fe atoms [14] during diffusion bonding is also responsible for the reduction in shear strength [22], though it may be not the main factor due to their small volume fraction. These voids were difficult to observe in SEM micrographs maybe owing to their sub-microscopic size, but it was evidenced by the fracture surfaces after shear testing as shown in Fig. 8.

All the joints fractured at Ti/F82H interface during shear testing and the fracture surfaces of the joints are given in Fig. 8. The fracture surface of the joint processed at low temperature is basically featureless (Fig. 8(a)). The discrete black islands attached on the fracture surface are Ti. When the joining temperature is raised to above 900 °C (Figs. 8(b) and (c)), transgranular brittle failure under a shear loading becomes evident by the presence of river patterns on fracture surfaces of both F82H and Ti sides. Within the cleavage planes, tongues are also observed, as shown in Figs. 8(b) and (c). The average composition of the cleavage facets (region A) on Ti side is Fe (~8 at. %), Cr (~1 at. %), and Ti (the balance), suggesting the existence of stabilized  $\beta$ -Ti. While the gray region B is comprised of Fe (~20 at. %), Cr (~2 at. %), and Ti (~80 at. %), FeTi +  $\beta$ -Ti phase mixture can be expected in this region. The white region C is Fe<sub>2</sub>Ti and

some oxide, with a composition of Fe (~62 at. %), W (~3 at. %), O (~6 at. %), Cr (~3 at. %), and Ti (the balance). Some W and Cr dissolved in this intermetallic phase. The presence of the Kirkendall voids which developed in the reaction phases can be observed on the surface as indicated by arrows in Fig. 8(c). The observed different phase mixtures on the fracture surfaces in the present work allow us to deduce that the failure occurred from the intermetallic phases (FeTi and Fe<sub>2</sub>Ti) and in some areas the fracture propagated in stabilized  $\alpha$ -Ti and  $\beta$ -Ti (close to intermetallics).

Microstructure of the interfaces can also be revealed by hardness testing. The hardness was evaluated on the polished cross-section of 900 °C joint and the result is shown in Fig. 9. W substrate shows a high hardness (~6.2 GPa). The W atom penetrated region between W and Ti slightly increases the hardness of this area (4.5 GPa) as compared with the more distant locations in Ti interlayer (~4.0 GPa). Meanwhile, the high hardness of  $\alpha$ - $\beta$  Ti is noted due to the solid solution strengthening. The fluctuation of the hardness value might be attributed to the mixed structure of  $\alpha$ - $\beta$  Ti. The stabilized  $\beta$ -Ti shows a high hardness value that is slightly higher than  $\alpha$ - $\beta$  Ti. A peak value (6.8 GPa) is located at Ti/F82H interface bond line. This can be justified by the formation of intermetallics in this region. The hardness value of F82H substrate is ~4.0 GPa and the fluctuant nature of data observed in F82H probably due to the penetration of Ti atom.

#### 4. Conclusions

The interfacial microstructure and mechanical properties of diffusion bonded

W/F82H joints using a Ti interlayer have been investigated and the following conclusions were drawn.

1) Cross-sectional examinations indicate that both the W/Ti and Ti/F82H interfaces were bonded well. The interdiffusion of chemical species is not evident at low joining temperature, but it is greatly enhanced above the  $\alpha$ - $\beta$  transformation temperature. The penetration of W atom into Ti leads to the formation of  $\alpha$ - $\beta$  Ti solid solution at the W/Ti interface. The diffusion path at the Ti/F82H interface was determined to be Ti/ $\alpha$ - $\beta$  Ti/stabilized  $\beta$ -Ti/ FeTi+Fe<sub>2</sub>Ti+Cr<sub>2</sub>Ti / $\alpha$ -Fe/F82H.

2) The strength increased firstly as the joining temperature was raised up to 900 °C and then decreased. The maximum shear strength of 113 MPa has been obtained for 900 °C joint.

3) The joints fractured at Ti/F82H interface during shear testing due to the incomplete interfacial deformation and limited interdiffusion occurred at the interface for the low joining temperature joints or the formation of brittle intermetallics for the high temperature joints.

4) The observed high hardness at both W/Ti and Ti/F82H interfaces is ascribed to the formation of solid solution and/or intermetallic phases.

## **Acknowledgements**

The authors would like to acknowledge the finance support partly from National Institute for Fusion Science, Japan. The authors are also grateful to Dr. Jung for technical assistance and Dr. Sharafat for English revision and discussion.

## References

- [1] R. Dux, V. Bobkov, N. Fedorczak, , K. Iraschko, A. Kallenbach, R. Neu, T. Pütterich, V.Rohde, ASDEX Upgrade Team. J. Nucl. Mater. 363-365 (2007) 112-116.
- [2] Z.J. Zhou, J. Du, S.S Song, Z.H. Zhong, C.C. Ge. J. Alloys Compd. 428 (2007) 146-150.
- [3] R.L. Klueh, A.T. Nelson. J. Nucl. Mater. 371 (2007) 37-52.
- [4] A. Hishinuma, A. Kohyama, R.L. Klueh, D.S. Gelles, W. Dietz, K. Ehrlich. J. Nucl. Mater. 258-263 (1998) 193-204.
- [5] T. Chehtov, J. Aktaa, O. Kraft. J. Nucl. Mater. 367-370 (2007) 1228-1232.
- [6] B.A. Kalin, V.T. Fedotov, O.N. Sevrjukov, A.N. Kalashnikova, A.N. Suchkova, A. Moeslang, M. Rohde. J. Nucl. Mater. 367-370 (2007) 1218-1222.
- [7] H. Greuner, H. Bolt, B. Böswirth, S. Lindig, W. Kühnlein, T. Huber, K. Sato, S. Suzuki. Fusion Eng. Des. 75-79 (2005) 333-338.
- [8] T. Hirose, K. Shiba, M. Ando, M. Enoda, M. Akiba. Fusion Eng. Des. 81 (2006) 645-651.
- [9] Z.H. Zhong, T. Hinoki, A. Kohyama. Mater. Sci. Eng. A, (2009), doi:10.1016/j.msea.2009.04.043.
- [10] H.Y. Yu, S.C. Sanday, B.B. Rath. J. Am. Ceram. Soc. 76 (1993) 1661-1664.
- [11] G. Rubin, A. Finel. J. Phys.: Condens. Matter, 7 (1995) 3139-3152.
- [12] S. Kundu, S. Chatterjee. Mater. Sci. Eng. A 425 (2006) 107-113.
- [13] N.F. Kazakov. Diffusion bonding of materials, Mir Publishers, Moscow, 1985.
- [14] M. Ghosh, S. Das, P.S. Banarjee, S. Chatterjee. Mater. Sci. Eng. A 390 (2005) 217-226.

- [15] V. Raghavan, Phase diagrams of ternary iron alloys, Vol. 1, ASM INTERNATIONAL, Metals Park, Ohio, 1987.
- [16] A. Fuji, K. Ameyama, T.H. North. J. Mater. Sci. 31 (1996) 819-827.
- [17] M. Ghosh, S. Kundu, S. Chatterjee, B. Mishra. Metall. Mater. Trans. A 36 (2005) 1891-1899.
- [18] Y.A. Shevchuk. Inorg. Mater. 40 (2004) 376-379.
- [19] S. Kundu, S. Chatterjee, D. Olson, B. Mishra. Metall. Mater. Trans. A 38 (2007) 2053-2060.
- [20] J.I. Akhter, M. Ahmad, M. Iqbal, M. Akhtar, M.A. Shaikh. J. Alloys Compd. 399 (2005) 96-100.
- [21] B. Aleman, I. Gutierrez, J.J. Urcola. Mater. Sci. Technol. 9 (2003) 633-641.
- [22] P. Liu, P. Yao, J. Liu. J. Alloys Compd. doi:10.1016/j.jallcom.2009.06.171.

## Table captions

[Table 1](#). Chemical compositions (wt. %) of the materials used in this work.

Alloy	Cr	C	N	P	S	Al	Si	V	Ti	Mn	Ta	W	O	Fe
F82H	7.84	0.09	0.007	0.003	0.001	0.001	0.07	0.19	0.004	0.1	0.04	1.98	0.01	Bal.
W	–	0.02	0.01	–	–	–	–	–	–	–	–	Bal.	0.02	–
Ti	–	0.02	–	–	–	–	–	–	Bal.	–	–	–	0.15	0.01

## Figure captions

**Fig. 1.** SEM micrograph of the cross-section of the specimen diffusion bonded at 900 °C for 1 h.

**Fig. 2.** SEM micrographs of the W/Ti interface of the specimens bonded at (a) 850 °C, (b) 900 °C, and (c) 950 °C for 1 h. The inset in each image was obtained at higher magnification.

**Fig. 3.** Intensity profiles of tungsten and titanium across the W/Ti interface for the joints bonded at (a) 850 °C, (b) 900 °C, and (c) 950 °C for 1 h.

**Fig. 4.** SEM micrographs of the Ti/F82H interface of the specimens bonded at (a) 850 °C, (b) 900 °C, and (c) 950 °C for 1 h. The inset in each image was obtained at higher magnification.

**Fig. 5.** Intensity profiles of titanium, iron, chromium, and tungsten across the Ti/F82H interface for the joints bonded at (a) 850 °C, (b) 900 °C, and (c) 950 °C for 1 h.

**Fig. 6.** XRD pattern of the fracture surface on Ti side for the joint bonded at 950 °C for 1 h.

**Fig. 7.** Shear strength vs. joining temperature of the W/Ti/F82H transition joint.

**Fig. 8.** Fracture surfaces of the joints bonded (a) at 850 °C, F82H side; (b) at 900 °C, Ti side; and (c) at 950 °C, Ti side.

**Fig. 9.** Hardness profile across the W/Ti/F82H interface for the joint bonded at 900 °C for 1 h.



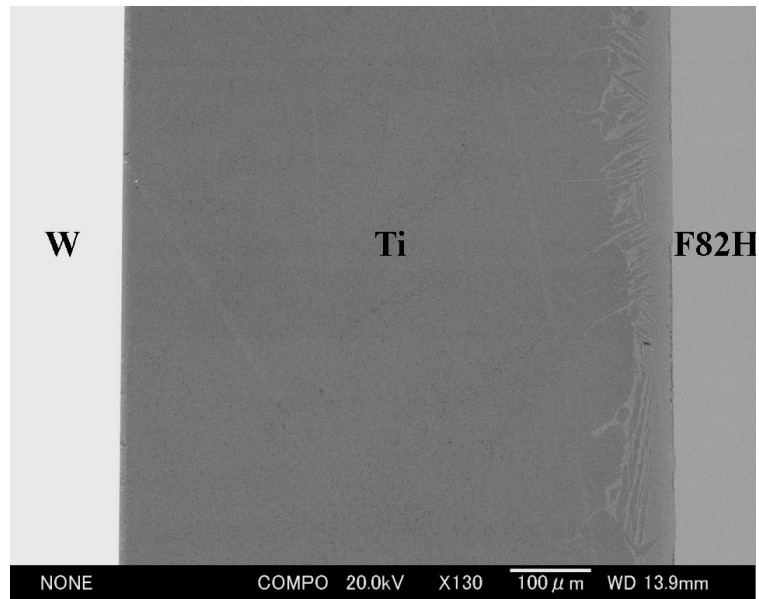


[Fig. 1.](#) SEM micrograph of the cross-section of the specimen diffusion bonded at 900 °C for 1 h.

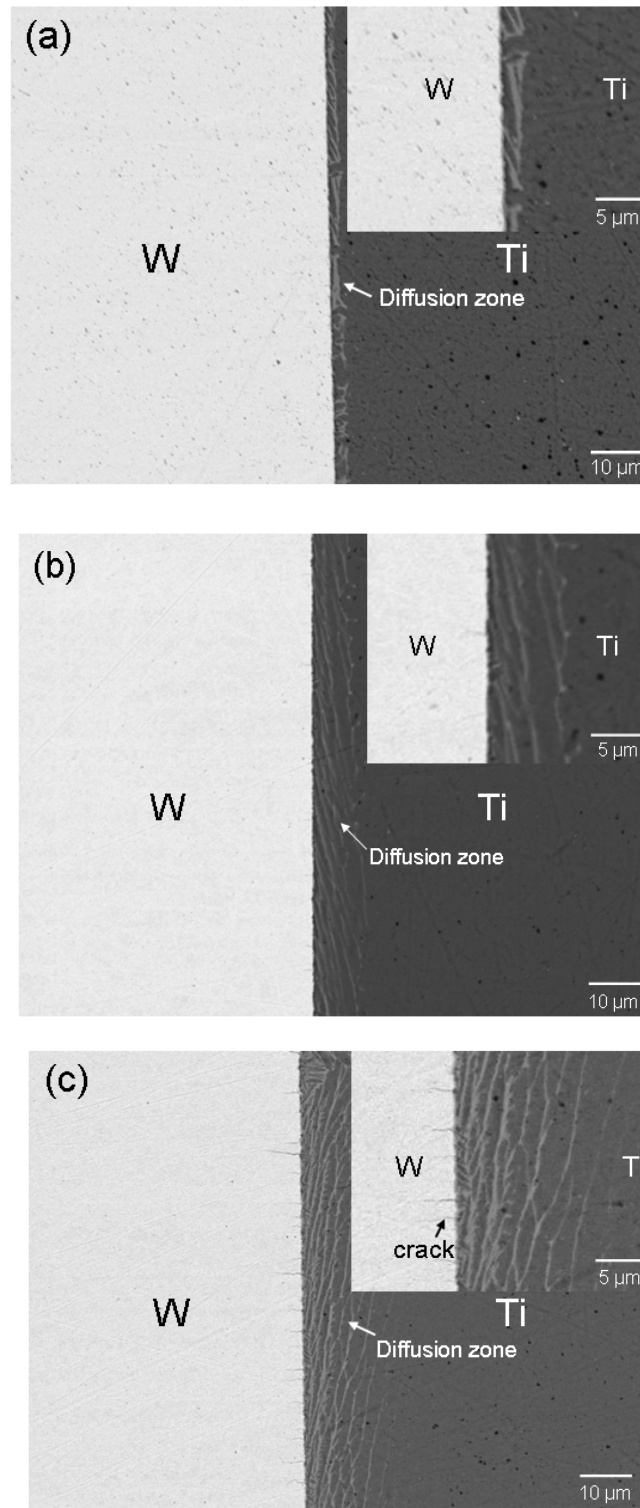


**Fig. 2.** SEM micrographs of the W/Ti interface of the specimens bonded at (a) 850 °C, (b) 900 °C, and (c) 950 °C for 1 h. The inset in each image was obtained at higher magnification.

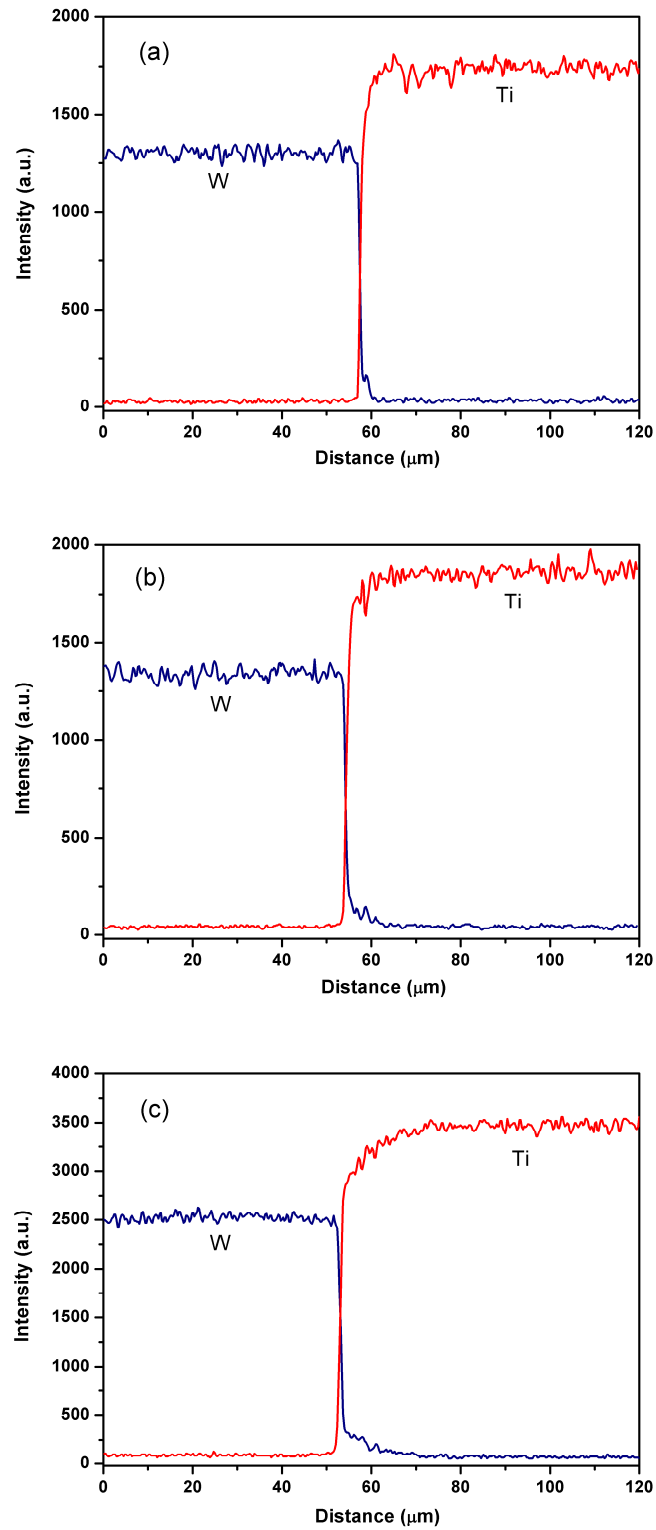


**Fig. 3.** Intensity profiles of tungsten and titanium across the W/Ti interface for the joints bonded at (a) 850 °C, (b) 900 °C, and (c) 950 °C for 1 h.

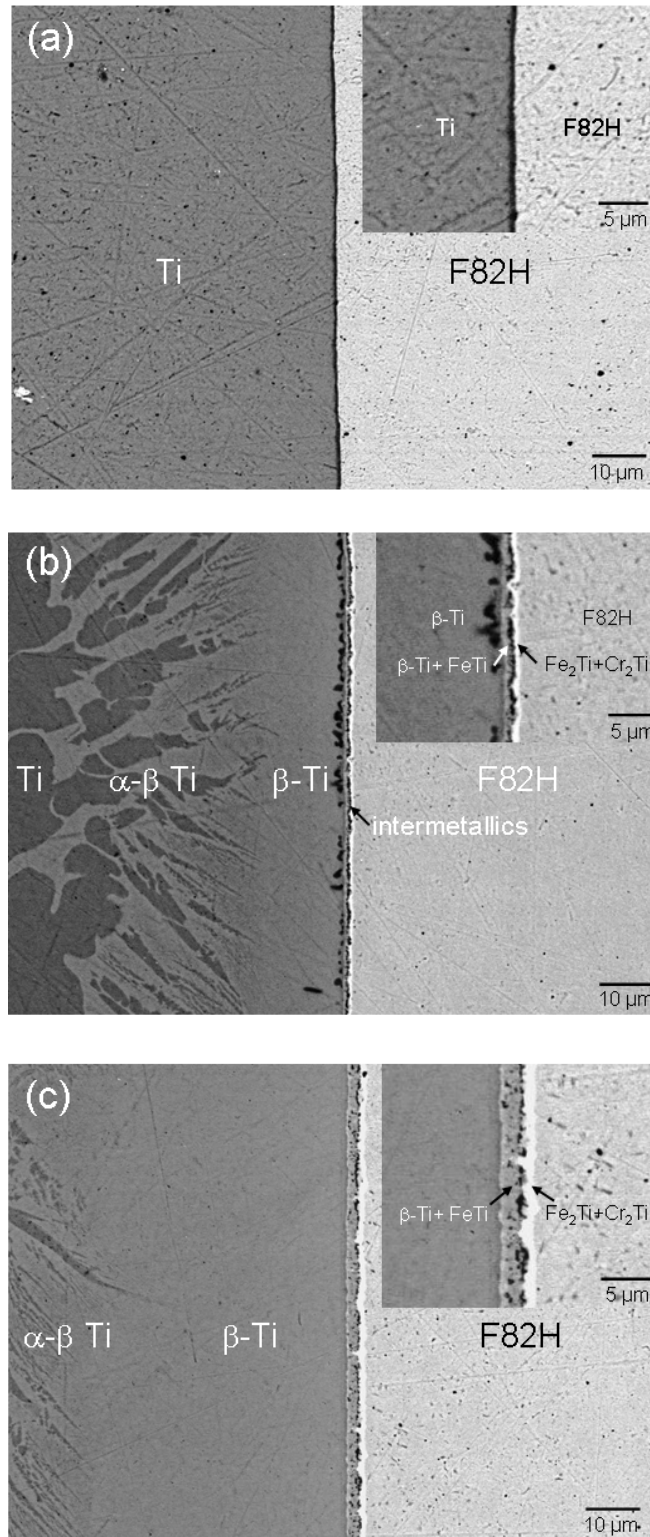


**Fig. 4.** SEM micrographs of the Ti/F82H interface of the specimens bonded at (a) 850 °C, (b) 900 °C, and (c) 950 °C for 1 h. The inset in each image was obtained at higher magnification.

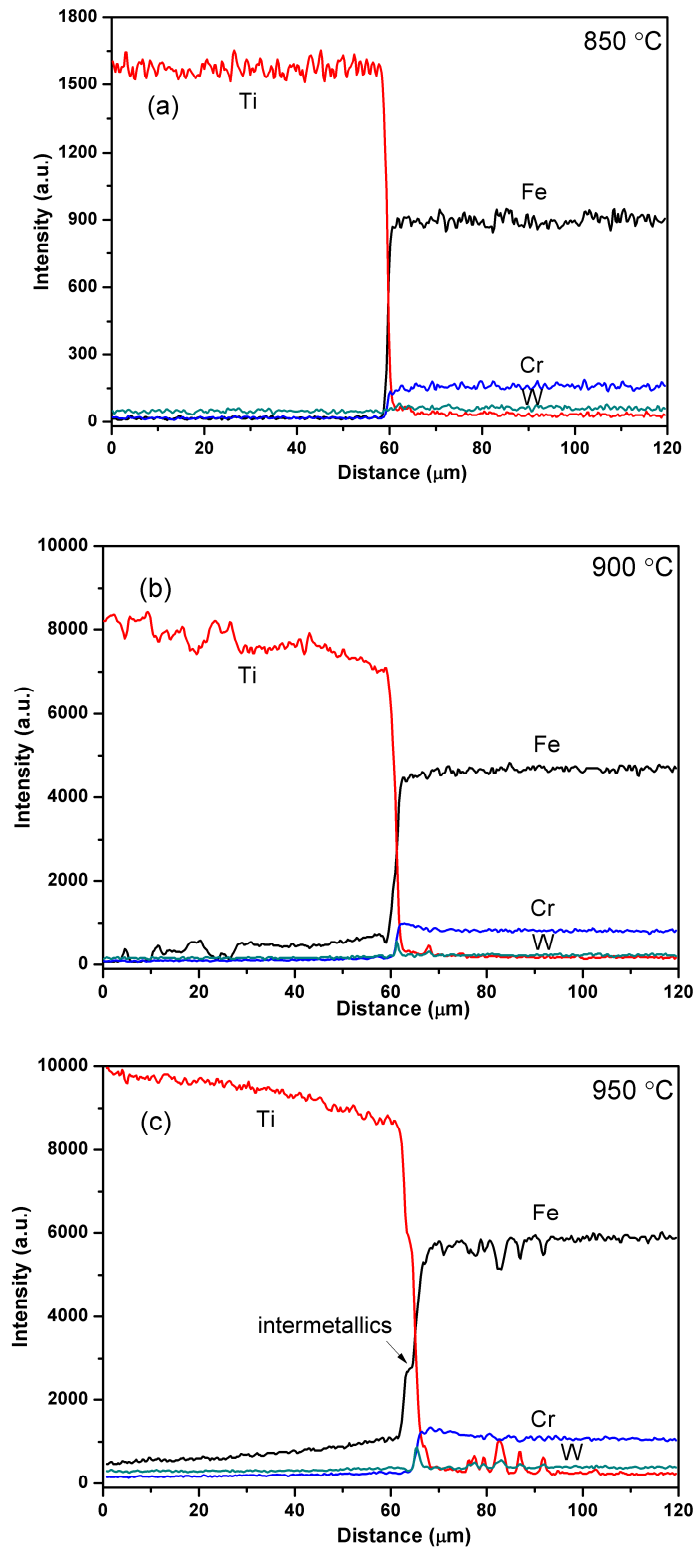


**Fig. 5.** Intensity profiles of titanium, iron, chromium, and tungsten across the Ti/F82H interface for the joints bonded at (a) 850 °C, (b) 900 °C, and (c) 950 °C for 1 h.

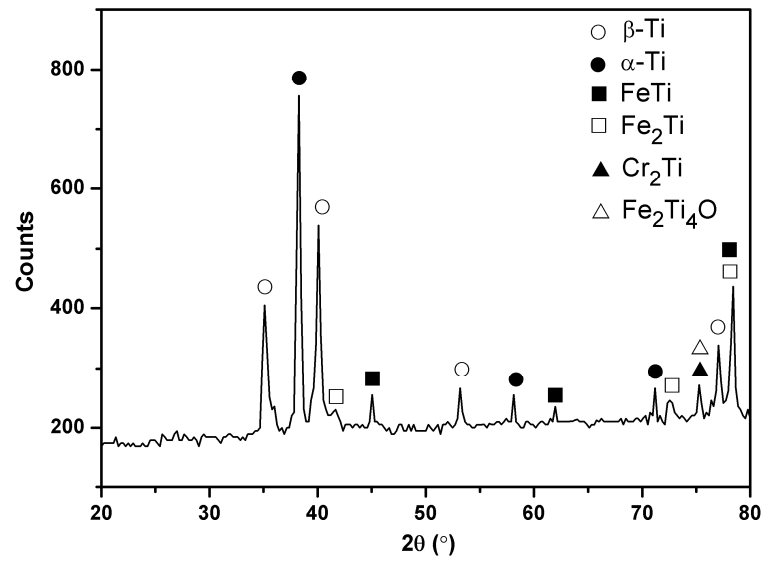


**Fig. 6.** XRD pattern of the fracture surface on Ti side for the joint bonded at 950 °C for 1 h.

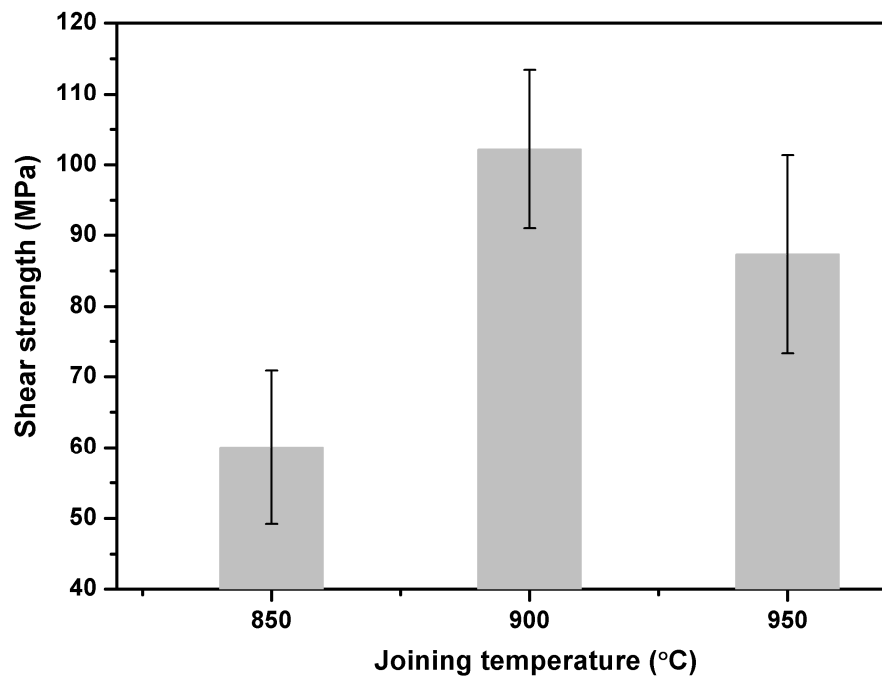
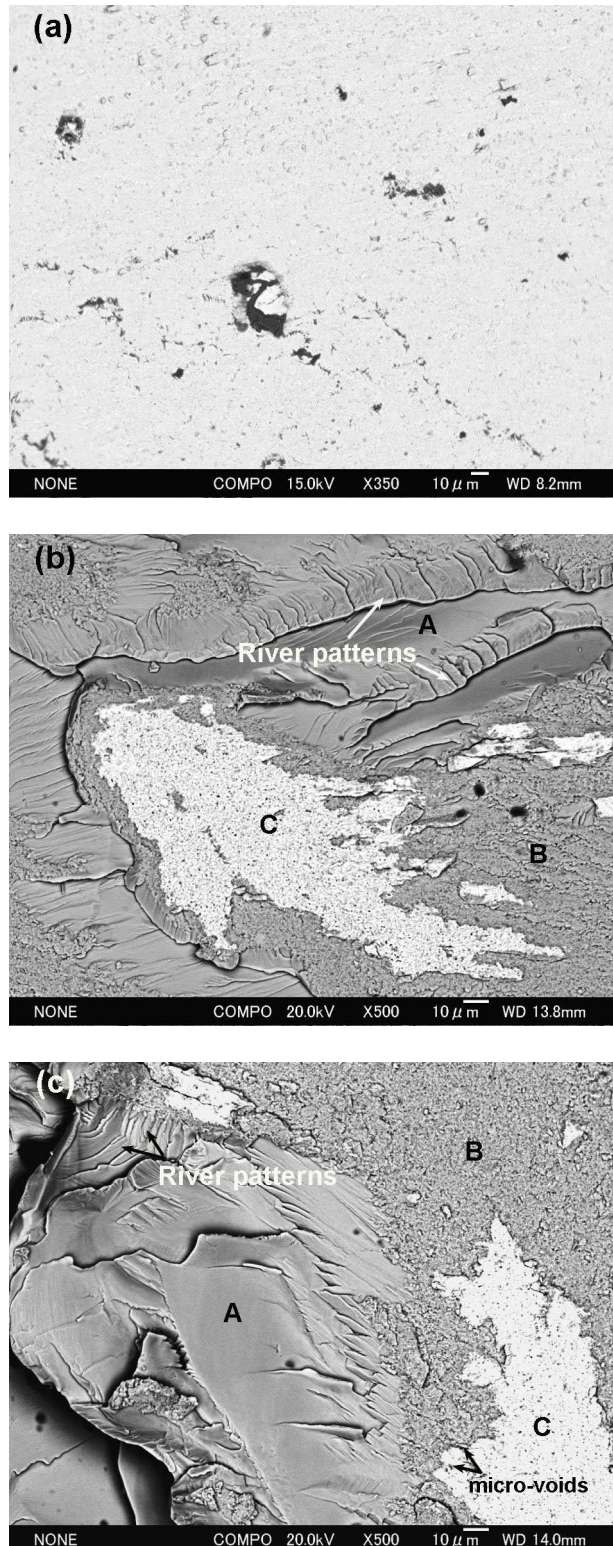


Fig. 7. Shear strength vs. joining temperature of the W/Ti/F82H transition joint.





**Fig. 8.** Fracture surfaces of the joints bonded (a) at 850 °C, F82H side; (b) at 900 °C, Ti side; and (c) at 950 °C, Ti side.



